

Co(salen) supported on graphene oxide for oxidation of lignin

Xue-Fei Zhou,^{1,2,3,4,5} Xu-Jie Lu⁵

¹Kunming University of Science and Technology, Kunming 650051, China

²State Key Laboratory Breeding Base-Key, Laboratory of Qinghai Province for Plateau Crop Germplasm Innovation and Utilization, Xining 810016, China

³Guangxi Key Laboratory of Petrochemical Resource Processing and Process Intensification Technology, Guangxi University, Nanning 530004, China

⁴Key Laboratory of Low-Grade Energy Utilization Technologies and Systems of Ministry of Education of China, Chongqing University, Chongqing 400044, China

⁵School of Tropical eco-Environment Protection, Hainan Tropical Ocean University, Sanya 572022, China

Correspondence to: X. F. Zhou (E-mail: lgdx602@tom.com)

ABSTRACT: Co(salen) was supported on graphene oxide (GO) (Co-GO) by covalently grafting. Spectroscopy analyses confirmed its successful synthesis. Co-GO demonstrated a high activity in the cleavage of β -O-4 linkage in lignin model compounds. The catalyst was also effective in depolymerizing an organosolv lignin polymer. The polymer residues were separated, and extensively analyzed by FTIR and NMR in order to understand the various structural changes of the polymer occurring versus catalyst. In catalytic oxidation, the β -O-4 ether linkages were cleaved and the side-chains were oxidized occurring in the polymer. The polymer was thus converted into smaller monomers called degradation products which were detected by GC-MS. The evolution of the polymer found that Co-GO exhibited a significant catalytic effect as compared with Co-NaY, Co-MCM-48, Co-SSZ-13. © 2016 Wiley Periodicals, Inc. *J. Appl. Polym. Sci.* **2016**, *133*, 44133.

KEYWORDS: biomimetic; catalysts; cellulose and other wood products; degradation

Received 5 March 2016; accepted 25 June 2016

DOI: 10.1002/app.44133

INTRODUCTION

Oxidation of lignin to various useful products is one of the most meaningful technology in the biomass conversion.¹ Much demands for fine chemicals have encouraged intense study into lignin transformation. Conventional metal salen complexes have been extensively used in the oxidation of lignin and lignin model compounds, but they inevitably have some limitations, such as easy deactivation because of polymeric formation and difficulty in separation of catalyst and product.^{2,3} Njiojob *et al.* reported that Co(salen) catalyst showed high conversion and selectivity for oxidation of β -O-4 lignin dimer models containing the S, G, and H subunits.⁴ Early studies found that metal salen complexes supported in zeolites significantly catalyzed the oxidation of lignin and lignin model compounds using O₂ or H₂O₂ as oxidants as compared to unsupported complexes.⁵⁻⁸ Therefore, encapsulation of metal salen complexes should be preferred to consider in oxidation of lignin.

Salen-type transition metal complexes are known to be used as biomimetic catalysts for a wide variety of organic catalytic reactions.⁹ For example, Co(salen)/oxidant is a highly excellent

catalytic system for oxidation of phenolic and nonphenolic β -O-4 aryl ether lignin model compounds.¹⁰⁻¹² However, their stability, selectivity, and recyclability should be improved by immobilization procedures for their wide application.¹³ The heterogenization of homogeneous catalysis has been considered to be an alternative approach because it allows the search for more robust catalysts. Covalent bond is a very effective method by anchoring effect for homogeneous metal salen complexes into supports. A lot of materials can be used as supports for catalysts, including natural mineral, adsorbent, glass, organic, etc.¹⁴⁻¹⁷ In particular, the immobilization of transition metal salen complexes onto supports constituted a promising alternatives for the selective degradation of lignin.

Graphene oxide (GO) as a precursor offers the high specific surface area and high chemical stability, therefore, it has been recognized as a promising candidate for supporting various transition metal complexes.^{18,19} Recently, Liu *et al.* synthesized a Fe- and N-functionalized graphene electrocatalysts. Fe complexes homogeneously deposited on GO (HD-FeN/G) were significantly superior to a FeN/G counterpart prepared via

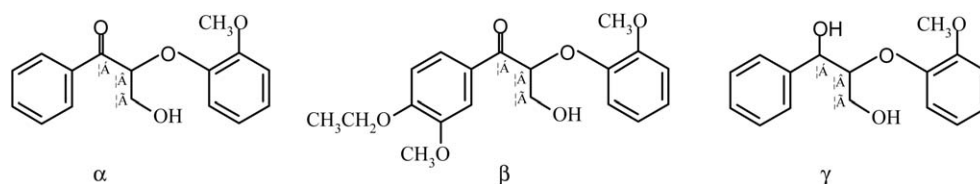


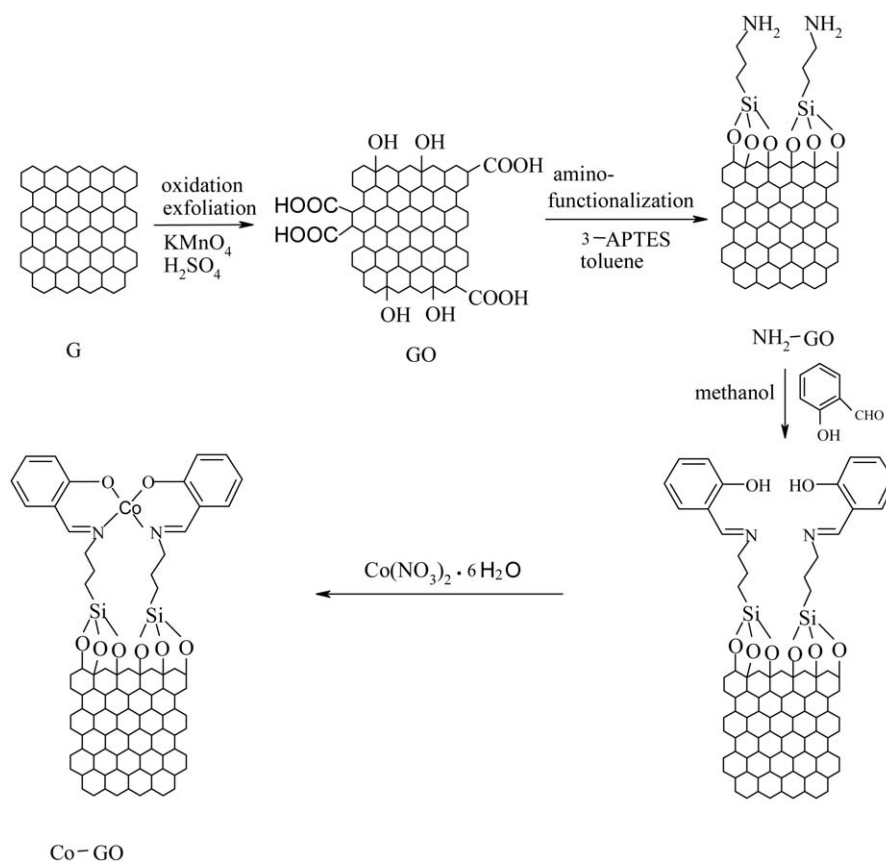
Figure 1. β -O-4 lignin model compounds.

traditional approach for the oxygen reduction reaction.²⁰ Su *et al.* reported the immobilization of Co(II), Fe(III), or VO(II) schiff base metal complexes on GO for the epoxidation of styrene.²¹ Li *et al.* successfully tethered MoO₂-salen complex onto amino-functionalized GO and tested its catalytic performance in the epoxidation of various alkenes using tert-butylhydroperoxide or hydrogen peroxide as oxidant, showing more active than its homogeneous analogue.²² This article reported the effect of grafting of Co(salen) onto GO as an efficient catalyst on the oxidation of organosolv lignin using air as the oxidant. To the best of our knowledge this is the first report of the application of metal salen complex immobilized on GO in the oxidation of lignin model compounds and lignin. In this article, organosolv lignin was considered because it could be representative of lignin in structure, providing a better understanding of the depolymerization of various technical lignin under different catalytic conditions.²³

EXPERIMENTAL

Materials and Samples

Chemicals. The following reagents were commercially available and were used as received: guaiacol (Sigma-Aldrich, 99.0%), 1,4-dioxane (Sinopharm Chemical Reagent, analytical grade), acetone (Sinopharm Chemical Reagent, analytical grade), ethyl acetate (Sinopharm Chemical Reagent, analytical grade), n-hexane (Sinopharm Chemical Reagent, analytical grade), anhydrous sodium sulfate (Sinopharm Chemical Reagent, analytical grade), dichloromethane (Sinopharm Chemical Reagent, analytical grade), methanol (Sinopharm Chemical Reagent, analytical grade), sodium borohydride (Sinopharm Chemical Reagent, analytical grade), potassium carbonate (Sinopharm Chemical Reagent, analytical grade), graphite powder (Sigma-Aldrich, 99.85%), potassium permanganate (KMnO₄, Sinopharm Chemical Reagent, analytical grade), acetic anhydride (Sinopharm Chemical Reagent, analytical grade), tetrahydrofuran (Sigma-



Scheme 1. Schematic procedure for synthesis of Co-GO.

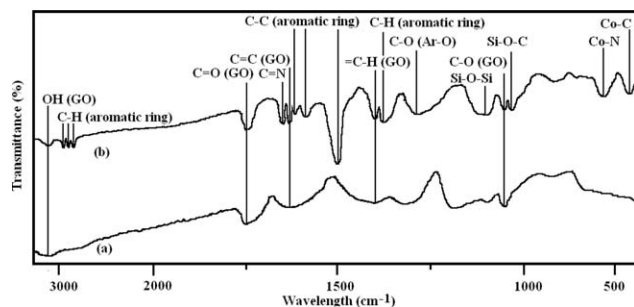


Figure 2. FTIR spectra of (a) GO, (b) Co-GO.

Aldrich, analytical grade), pyridine (Sinopharm Chemical Reagent, $\geq 99.9\%$), cyclohexanol (Sigma-Aldrich, 99.0%), sulfuric acid (H_2SO_4 , Sinopharm Chemical Reagent, analytical grade), 2-chloro-4,4,5,5-tetramethyl-1,3,2-dioxaphospholane (Sigma-Aldrich, 95%), CDCl_3 (Sigma-Aldrich, 99.8% atom D), DMSO-d_6 (Sigma-Aldrich, 99.9% atom D), hydrogen peroxide (H_2O_2 , Sinopharm Chemical Reagent, analytical grade), hydrochloric acid (HCl, Sinopharm Chemical Reagent, analytical grade), 3-aminopropyltriethoxysilane (3-APTES, Sigma-Aldrich, 99%), $\text{Co}(\text{NO}_3)_2 \cdot 6\text{H}_2\text{O}$ (Sinopharm Chemical Reagent, analytical grade). The other chemicals used in the synthesis of lignin model compounds were reagent grade and were used as supplied by Aldrich Scientific.

Synthesis of Lignin Model Compounds. Lignin model compound a [Figure 1(a)]: Formaldehyde (9.54 mmol) reacted with 2-(2-methoxyphenoxy)-1-phenylethanone (6.20 mmol) in the presence of K_2CO_3 (7.44 mmol) in $\text{CH}_3\text{CH}_2\text{OH}$ -acetone solution (1:1, 45 mL) for 2 h at room temperature. 2-(2-Methoxyphenoxy)-1-phenylethanone was synthesized by literature.²⁴ The mixture was evaporated in vacuum and extracted with CH_2Cl_2 . The appropriate fractions were collected via purifying with silica gel chromatography (2:1 hexane-ethyl acetate), evaporating, and re-precipitating with CH_2Cl_2 /hexane. $^1\text{H-NMR}$ (400 MHz, CDCl_3): δ 3.02 (OH, t, 1H), 3.84 (OCH_3 , s, 3H), 4.08 (HOCH_2 , m, 2H), 5.42 (CH, t, 1H), 6.84 (Ar-H, t, 1H), 6.91 (Ar-H, d, 2H), 7.03 (Ar-H, t, 1H), 7.47 (Ar-H, t, 2H), 7.62 (Ar-H, t, 1H), 8.05 (Ar-H, d, 2H). $^{13}\text{C-NMR}$ (100 MHz, CDCl_3): δ 55.97 (OCH_3), 63.56 (HOCH_2), 85.04 (CH), 112.53, 119.02, 121.37, 123.96, 128.93, 133.94, 135.13, 147.06, 150.73, 196.73 (C=O). C, 68.35%; H, 6.07% (theoretically: C, 68.31%; H, 6.09%).

Lignin model compound b [Figure 1(b)] was synthesized by literature methods²⁵:

Lignin model compound c [Figure 1(c)]: Methyl 3-hydroxy-2-(2-methoxyphenoxy)-3-phenylpropanoate (4.5 mmol) was reduced by NaBH_4 (22.5 mmol) in a $\text{THF}/\text{H}_2\text{O}$ (3 : 1, 45 mL) solution for 22 h at room temperature. Ethyl acetate (75 mL) was then added following the addition of a saturated NH_4Cl (75 mL). The organic layer was collected, and the aq. layer was extracted using diethyl ether (2×75 mL). The combined organic layers were dried over MgSO_4 , evaporated, dried in vacuum. $^1\text{H-NMR}$ (600 MHz, CDCl_3): δ 2.94 (CH_2OH , t, 1H), 3.63–3.67 (CHHOH , m, 1H), 3.77 (CHOH, d, 1H), 3.86 (OCH_3 , s, 3H), 3.92–3.96 (CHHOH , m, 1H), 4.17–4.24 (CHCH_2 , m, 1H), 5.06

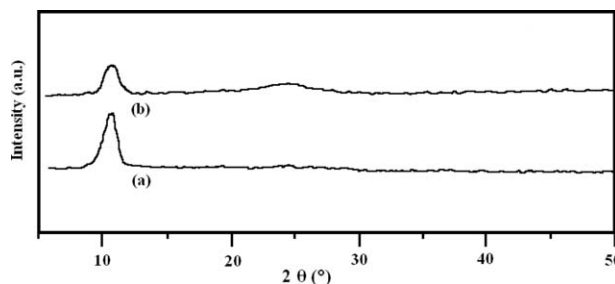


Figure 3. XRD spectra of (a) GO, (b) Co-GO.

(CHOH, ps t, 1H), 6.86–6.97 (Ar-H, m, 3H), 7.08 (Ar-H, t, 1H), 7.27 (Ar-H, t, 1H), 7.39 (Ar-H, t, 2H), 7.38 (Ar-H, d, 2H). $^{13}\text{C-NMR}$ (150 MHz, CDCl_3): δ 55.96 (OCH_3), 60.69 (CH_2OH), 72.96 (CHOH), 87.36 (CHCH_2). C, 69.85%; H, 6.69% (theoretically: C, 70.06%; H, 6.61%).

Methyl 3-hydroxy-2-(2-Methoxyphenoxy)-3-Phenylpropanoate: Methyl 2-(2-Methoxy phenoxy) acetate (30 mmol) was mixed with THF (90 mL) and cooled to -78°C . Methyl 2-(2-methoxyphenoxy) acetate was synthesized by literature.²⁶ Cyclohexane and benzaldehyde (30 mmol) were then added. The saturated aq. NH_4Cl (75 mL) was added and the mixture reacted for 2 h at -78°C under Ar. The organic layers were collected, and the aq. layer was extracted with ethyl acetate (3×75 mL). The combined organic layers were dried over MgSO_4 , evaporated, and purified via silica gel chromatography (2:1 hexane-ethyl acetate). The appropriate fraction was collected, rotary evaporated, treated with CH_2Cl_2 /hexane (1:10), precipitated, washed with hexane (2×15 mL), and dried in vacuum.

Organosolv Lignin. Organosolv lignin was extracted from sanded eucalyptus sawdust with 95% ethanol/5% 4M HCL (v/v) according to procedures reported in literature.²⁷

Co(salen) Supported on GO (Co-GO). Co(salen) catalyst was supported on GO using a postgrafting method as shown in Scheme 1.²² $\text{NH}_2\text{-GO}$ was mixed well with salicylaldehyde, the resulting solid was refluxed with $\text{Co}(\text{NO}_3)_2 \cdot 6\text{H}_2\text{O}$ to give the Co-GO. $\text{NH}_2\text{-GO}$ was obtained by reaction between GO and 3-aminopropyltriethoxysilane (3-APTES). GO was prepared by the

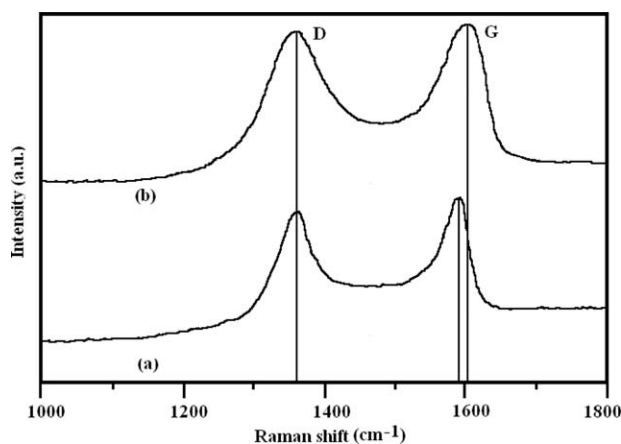


Figure 4. Raman spectra of (a) GO, (b) Co-GO.

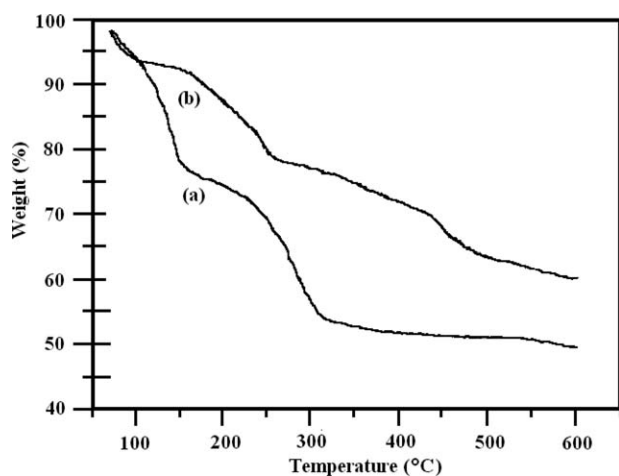


Figure 5. TGA spectra of (a) GO, (b) Co-GO.

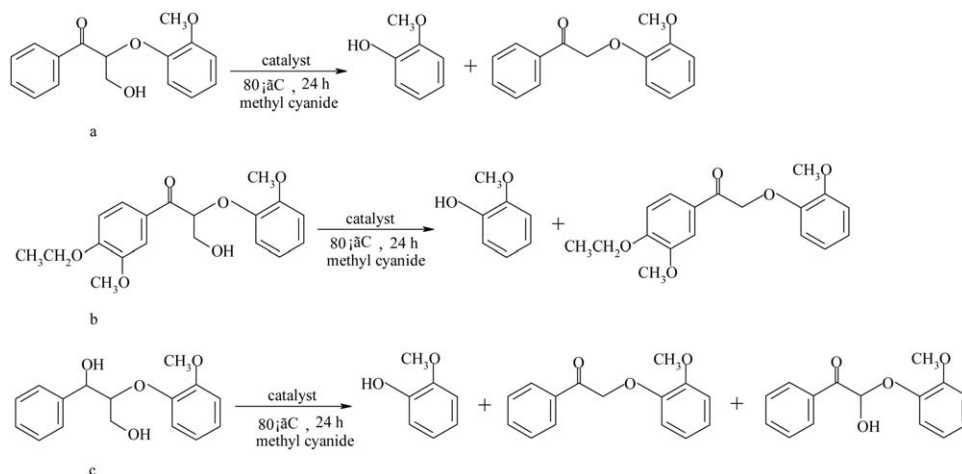
oxidation of graphite powder with potassium permanganate (KMnO_4) using the modified Hummers method.²⁸

Catalytic Experiments

Oxidation of lignin model compound or organosolv lignin was conducted at 80 °C for 24 h in sealed vials using air as oxidant. In a typical experiment, 100 mg lignin, 100 mL acetonitrile/THF mixture (10:1), and 10 wt % Co-GO (calculated on the lignin) were used. For comparison, the other catalysts, Co-NaY, Co-MCM-48, Co-SSZ-13, Co(salen), were also tested in the amount of Co(salen) as used in Co-GO test. Upon completion, the reaction mixture was then filtered into the liquid and the solid (catalyst). The catalyst was washed twice with acetonitrile and dried at 50 °C for reuse. The liquid was evaporated to dryness and analyzed by FTIR, NMR, and GPC to characterize the structural changes in the lignin, respectively.

Oxidation of lignin model compound was carried out in methyl cyanide. The amount of catalyst used was 10% mol Co(salen) to the lignin model compound.

Additional control experiments, in which catalyst was absent, were also carried out for evaluating catalyst.



Scheme 2. Catalyzed degradation of lignin model compound.

Analyses

X-ray Diffraction Analysis for Catalyst. Powder X-ray diffraction (XRD) pattern of Co-GO was recorded using a Shimadzu XRD-6000 diffractometer equipped with Ni-filtered, CuK α radiation.

Thermogravimetric Analysis for Catalyst. Thermogravimetric analysis (TGA) of Co-GO was performed using a Baehr-Thermo TGA 503 analyzer in a nitrogen stream with a heating rate of 10 °C/min.

Specific Surface Area Analysis for Catalyst. The specific surface area of Co-GO was determined by BET method using a Micromeritics ASAP-2020 system.

Raman Spectra Analysis for Catalyst. Raman spectrum of Co-GO was obtained using a confocal micro-Raman spectrometer (Almega XR).

Cobalt Content Analysis for Catalyst. Cobalt content for catalyst was performed by ICP-AES (Spectro Blue).

FTIR Analysis for Catalyst and Lignin. FTIR analyses were performed in KBr pellets using a Bruker Tensor 27 FTIR spectrometer in order to obtain structural information. The data were acquired in the range of spectral range from 400 to 4000 cm^{-1} with a resolution of 4 cm^{-1} .

NMR Analysis for Lignin. HMBC NMR spectra were obtained with a Bruker DRX500 500 MHz spectrometer. The accurate determination of phenolic moieties in the lignin were performed with the ^{31}P NMR spectra using 2-chloro-4,4,5,5-tetramethyl-1,3,2-dioxaphospholane as phosphitylation agent, and cyclohexanol acting as internal standard according to the previously reported procedure.^{29,30}

GC-MS Analysis for Degradation Products from Lignin. After reaction, the liquid filtered from the reaction mixture was added with isopropylphenol as internal standard, and reacted with BSTFA (N,O-bis(trimethylsilyl)trifluoroacetamide) containing TMSCl (trimethylchlorosilane) at 70 °C for 30 min. A sample of 1 μL was injected into a VF5-ms capillary column (30 m \times 0.25 mm \times 0.25 μm , Varian, Palo Alto) in splitless mode. The GC-MS analysis for degradation products from the lignin was

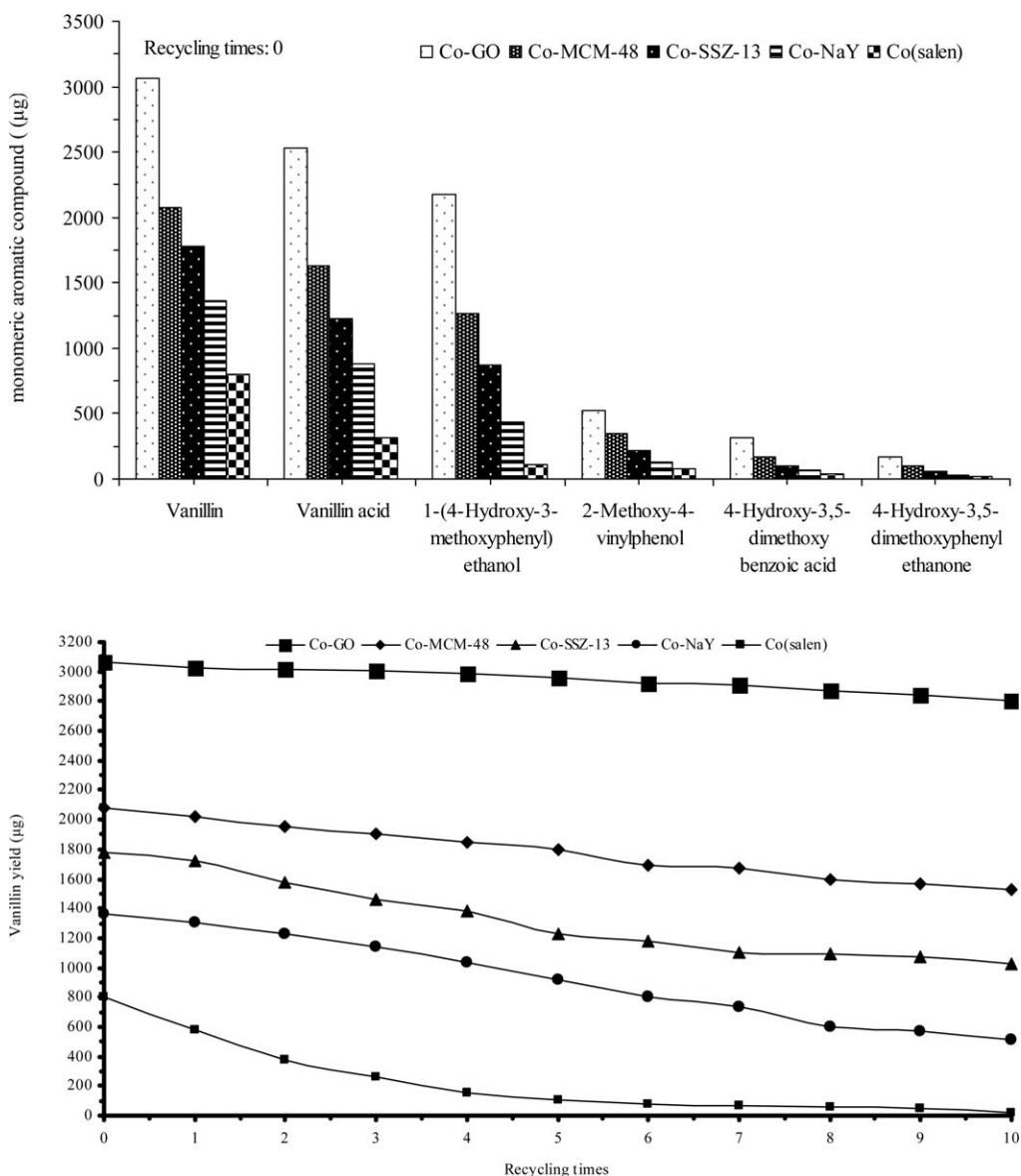


Figure 6. Vanillin yield-recycling times profile in oxidation of the lignin by Co-GO, Co-MCM-48, Co-SSZ-13, Co-NaY, and Co(salen).

performed on an Agilent 7890A gas chromatograph/5975 mass spectrometer system using He as the carrier gas (1.0 mL min^{-1}). The GC oven worked in the range of temperature from $60 \text{ }^\circ\text{C}$ (5 min initial delay) to $280 \text{ }^\circ\text{C}$ (held 20 min) with a $10 \text{ }^\circ\text{C min}^{-1}$. Compound identification was performed by comparison to the NIST database entries or literature data and was further confirmed by the model compounds using retention time if available. Quantification was performed in internal standard calibration mode using isopropyl phenol.

RESULTS AND DISCUSSION

Characterization of Co-GO

FTIR. FTIR spectra showed several characteristic groups of GO at peaks 3062 cm^{-1} (OH), 1720 cm^{-1} (C=O), 1625 cm^{-1} (C=C), 1390 cm^{-1} (C-H), 1040 cm^{-1} (C-O) [Figure 2(a)], corresponding to hydroxyl, carboxyl, and epoxy groups in GO. The bonds of Si-O-Si and Si-O-C were successfully found

to be formed after Co(salen) have been covalently grafted onto the GO surface, as confirmed by the bands at 1103 –, 1025 cm^{-1} in FTIR spectra [Figure 2(b)]. Similarly, the successful grafting of Co(salen) onto the GO surface was further confirmed by the bands at 2972 – $2880/1375 \text{ cm}^{-1}$ (C-H in aromatic ring), $1610/1580/1500 \text{ cm}^{-1}$ (C-C in aromatic ring), 1635 cm^{-1} (C=N), 1284 cm^{-1} (C-O/Ar-O), 568 cm^{-1} (Co-N), 470 cm^{-1} (Co-O) [Figure 2(b)].^{30,31}

X-ray Diffraction. XRD analysis was performed on GO, Co-GO, as shown in Figure 3. After the oxidation treatment, the diffraction peak of crystal plane of sample moved from peak at 25.6° to peak at 10.4° , showing the introduction of oxygen-containing groups, such as hydroxyl, carboxyl, epoxy between the graphite layers. In addition, as shown in Figure 3(b), the characteristic diffraction peak of functionalized oxygen-containing groups of GO appeared at about 25.0° when

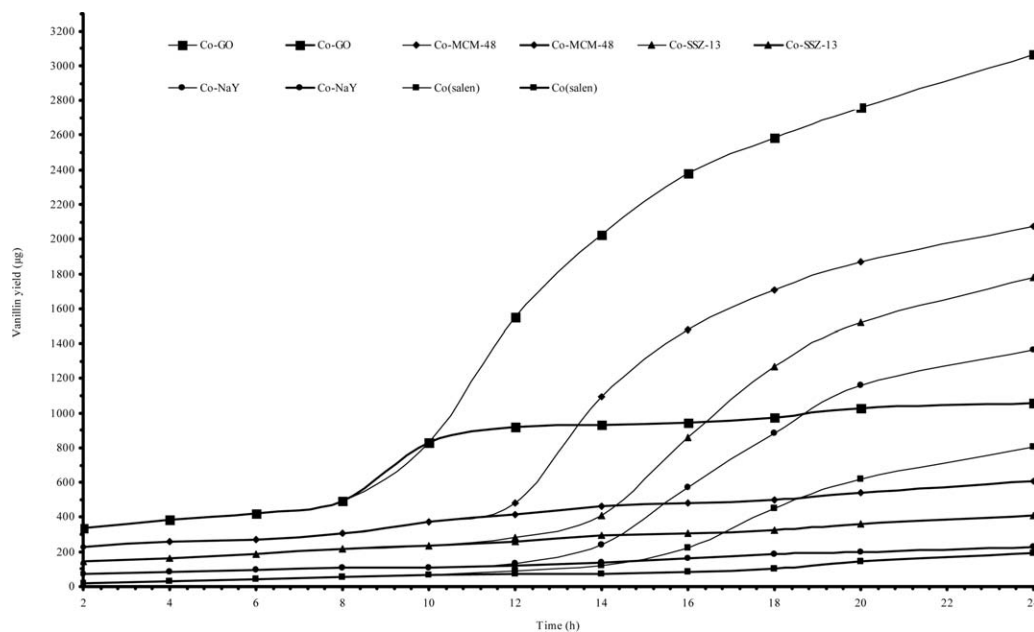


Figure 7. Vanillin yield-time profile in oxidation of the lignin by Co-GO, Co-MCM-48, Co-SSZ-13, Co-NaY, and Co(salen).

compared with GO, this was because of the grafting of Co(salen) onto the GO surface.^{32,33}

Raman. The samples were characterized by Raman spectroscopy, the spectra were shown in Figure 4. Raman data indicated that the grafting process caused the D band to broaden. The G band of Co-GO at 1605 cm^{-1} showed a shift as compared with the GO. The shift and band broadening of Raman modes resulted from the grafting effect by the introduction of oxygen-containing groups.³⁴

Thermogravimetric Analysis. Figure 5 showed the TGA spectra of GO and Co-GO. For GO sample, there were two distinct steps of mass loss in the range of measuring temperature. The mass loss in the range of temperature below $150\text{ }^{\circ}\text{C}$ was mainly caused by the evaporation of GO adsorbed water. The mass loss in the range of $200\text{--}300\text{ }^{\circ}\text{C}$ was possibly because of the thermal decomposition of oxygenic groups present in GO, and thus producing CO, CO_2 , and H_2O .³⁵ When Co(salen) was grafted onto GO (Co-GO), the mass loss below $250\text{ }^{\circ}\text{C}$ was because of a small amount of adsorbed water. The second mass loss was observed between $250\text{ }^{\circ}\text{C}$ and $450\text{ }^{\circ}\text{C}$ as a result of the thermal decomposition of labile oxygenic groups.³⁶ In the third stage in the range of $450\text{--}600\text{ }^{\circ}\text{C}$, Co(salen) was decomposed, which resulted in a significant mass appeared.³⁷

As measured using thermal analysis, after the grafting of Co(salen) onto GO, most of the functional groups of GO have been stabilized, so that Co-GO has a good thermal stability.

Degradation of Lignin Model Compound

The degradation of lignin model compounds was carried out using these catalysts. Co-GO was found to be the most active among the catalysts, degrading 90% of the lignin model compounds to produce various degradation products through the $\beta\text{--O--4}$ cleavage and a small degree of alcohol oxidation at the side chain (Scheme 2). By contrast, the increased reactivity of

Co-GO could be attributed to the GO offering a high chemical stability to ensure cobalt-based intermediates remaining as catalytically active monomeric species.³⁸

The benzyl alcohol oxidation obtained in model degradation was interesting not only for its reactivity, but also because the oxidation did not occur when the group was carbonyl at the same C-position. On the other hand, the lignin model compound b (Scheme 2) was degraded proceeding with the lower selectivity and efficiency than the model a under the same reaction conditions.

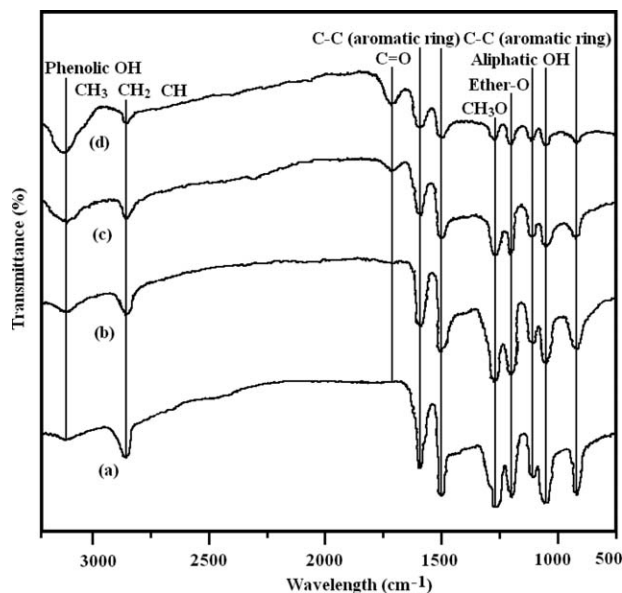


Figure 8. FTIR spectra of (a) lignin, (b) lignin residue after control treatment, (c) lignin residue after Co(salen) treatment, (d) lignin residue after Co-GO treatment.

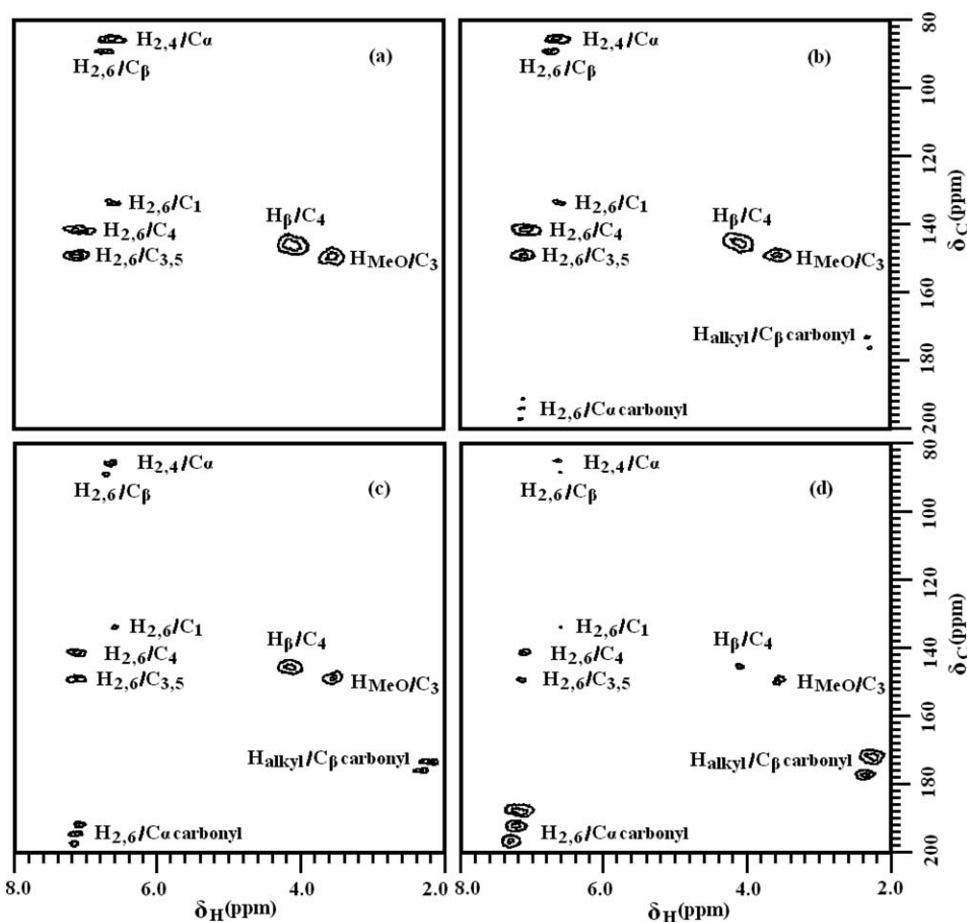


Figure 9. HMBC spectra of (a) lignin, (b) lignin residue after control treatment, (c) lignin residue after Co(salen) treatment, (d) lignin residue after Co-GO treatment.

Degradation of Lignin

Degradation Product from the Lignin. Degradation products were detected by GC-MS for the oxidation of the lignin. The lignin was converted into vanillin, vanillin acid, 1-(4-hydroxy-3-methoxyphenyl) ethanol, and other monomeric aromatic compounds. Vanillin was found to be the main compound in the degradation products. The blank test showed negligible effect on the oxidation of the lignin when catalyst was not added, whereas air exhibited a significant effect when catalyst was used in the oxidation of the lignin. In addition, the higher yield of compounds were obtained when heterogeneous catalysts were used as compared with homogeneous Co(salen). The balance between mono- and bi-nuclear complexes can be shifted towards the catalytically more active

species by the uniform dispersing of Co(salen) onto the external surface of support.³⁹ Moreover, Co-GO exhibited the better catalytic effect in the lignin oxidation than the other catalysts supported in NaY, MCM-48, SSZ-13, as shown in Figure 6. For example, when the same weight of Co(salen) was used, Co-MCM-48 produced 2076 μg vanillin, Co-SSZ-13 produced 1781 μg vanillin, Co-NaY produced 1366 μg vanillin, while Co-GO produced 3067 μg vanillin, since the layer structure of GO provided more voids for dispersion and approaching (S_{BET} : Co-GO 478 m^2/g , Co-MCM-48 362 m^2/g , Co-SSZ 13 328 m^2/g , Co-NaY 273 m^2/g).⁴⁰

After the reaction, the catalysts were recovered from the reaction mixture by filtration and reused in order to evaluate their

Table I. OH Content in the Lignin and Lignin Residue by ^{31}P NMR

| Groups | Chemical shift (ppm) | Concentration (mmol OH/g) | | | |
|--------------|----------------------|---------------------------|--|--|--------------------------------------|
| | | Lignin | Lignin residue after control treatment | Lignin residue after Co(salen) treatment | Lignin residue after Co-GO treatment |
| Aliphatic OH | 150.0-145.0 | 5.29 | 5.02 | 4.08 | 3.14 |
| Phenolic OH | 140.5-138.6 | 1.46 | 1.62 | 2.78 | 5.52 |
| Carboxyl OH | 136.0-134.0 | 0.08 | 1.06 | 1.82 | 3.16 |

stability in recycling experiments. The results were shown in Figure 6. It was clear that all the encapsulated catalysts were relatively stable in the recycling process. Furthermore, the experiments confirmed the significant performance of Co-GO in increasing the reuse as compared with the other encapsulated catalysts, which indicated that M(salen) complex supported into GO could become an important catalyst in the catalytic process for lignin depolymerization.⁴¹ The leaching experiments performed with Co-GO, Co-MCM-48, Co-SSZ-13, Co-NaY, and Co(salen) further confirmed their stability during the catalytic process. The catalyst was removed by filtration after 10 h and the reaction was allowed to continue. As shown in Figure 7, it was obviously found little reactions were further observed after the heterogeneous catalyst was removed from the reaction mixture. This indicated that the heterogeneous catalyst was not leaked into the solution in the oxidation of the lignin.

Structural Analysis for the Lignin Degradation. Control experiment, in which catalyst was absent, was conducted simultaneously. Upon completion, each of the resulting mixtures was evaporated to dryness and analyzed by FTIR and NMR to characterize the change in functional groups.

In the case of FTIR, characteristic structure was observed for lignin (phenolic HO, CH₃, CH₂, CH, aromatic ring, CH₃O, aliphatic OH, ether-O) in Figure 8(a).⁴² In addition, guaiacyl groups were distinctively characterized by ether-O bond at 1188 cm⁻¹ and aromatic C-H bond 843 cm⁻¹, respectively. By comparison, FTIR spectra of the polymer residue showed the increase of C=O bonds (1710 cm⁻¹), phenolic OH (3157 cm⁻¹), and the decrease of the intensities of CH₃/CH₂/CH (2875 cm⁻¹), aromatic ring (1593-, 1500-, 843 cm⁻¹), CH₃O (1267 cm⁻¹), ether-O (1188 cm⁻¹), and aliphatic OH (1110-, 1062 cm⁻¹) units.

Figure 9 was a brief show of the HMBC NMR spectra for the lignin, and ³¹P NMR determined a number of important phenolic structural features in lignin including.⁴³ The quantification of the various phenolics obtained by ³¹P NMR was shown in Table I. The ³¹P NMR experiments indicated an increase of the amount of phenolic and carboxylic functions, but also a decrease of the amount of aliphatic hydroxyl groups from the polymer sample to the Co-GO sample. This was the result of the progressive removing of β-O-4, methoxyl groups and the oxidation of side-chain groups in the polymer structure. HMBC experiments confirmed this finding since we can observed the decrease of methoxy groups on aromatic rings and C_β/H₄ in β-O-4 linkages in Figure 9. Furthermore, we observed that the signals of H_{alkyl}/C_β carbonyl, H_{2,6}/C_α carbonyl were even more intense, the signals of H_{2,6}/C_β, H_{2,4}/C_α in aliphatic chains (CH₃, CH₂, CH) were weaker, in the polymer residues. Thus, we can proposed that the oxidation of the aliphatic groups leading to the formation of carbonyl, and the cleavage of β-O-4 and the demethylation of methoxyl with the formation of phenolic OH. The support of Co(salen) on the GO has increased dramatically the oxidation of polymer.

CONCLUSIONS

Co(salen) was successfully supported on GO (Co-GO). In addition, Co-GO showed a significant reactivity observed in the

catalyzed oxidation of lignin model compounds or organosolv lignin as compared with the catalysts immobilized in the conventional supports. The lignin reaction was explained using FTIR, NMR, and GC-MS. Considering the catalytic effect obtained in this article, further study is thus worth to be considered in biomass oxidation using Co-GO as catalyst.

ACKNOWLEDGMENTS

This work was supported by the National Natural Science Foundation of P. R. China (No. 21166011), the Open Research Foundation of State Key Laboratory Breeding Base-Key Laboratory of Qinghai Province for Plateau Crop Germplasm Innovation and Utilization (2014-12), the Open Research Foundation of Guangxi Key Laboratory of Petrochemical Resource Processing and Process Intensification Technology of Guangxi University (2014K002), the Open Research Foundation of Key Laboratory of Low-grade Energy Utilization Technologies and Systems of Ministry of Education of China of Chongqing University (LLEUTS-201605).

REFERENCES

1. Mafakheri, F.; Nasiri, F. *Energy Policy* **2014**, *67*, 116.
2. Ambrose, K.; Hurisso, B. B.; Singer, R. D. *Can. J. Chem.* **2013**, *91*, 1258.
3. Lange, H.; Decina, S.; Crestini, C. *Eur. Polym. J.* **2013**, *49*, 1151.
4. Njiojob, C. N.; Rhinehart, J. L.; Bozell, J. J.; Long, B. K. *J. Org. Chem.* **2015**, *80*, 1771.
5. Zhou, X. F. *Environ. Prog. Sustain.* **2015**, *34*, 1120.
6. Zhou, X. F. *RSC Adv.* **2014**, *4*, 28029.
7. Zhou, X. F. *J. Appl. Polym. Sci.* **2014**, *131*, DOI: 10.1002/app.40809.
8. Zhang, N.; Zhou, X. F. *J. Mol. Catal. A Chem.* **2012**, *365*, 66.
9. Gu, Z. Y.; Park, J.; Raiff, A.; Wei, Z.; Zhou, H. C. *Chemcatchem* **2014**, *6*, 67.
10. Haikarainen, A. Metal-Salen Catalysts in the Oxidation of Lignin Model Compounds, Ph.D. Thesis, University of Helsinki; **2005**.
11. Cedeno, D.; Bozell, J. J. *Tetrahedron Lett.* **2012**, *53*, 2380.
12. Badamali, S. K.; Luque, R.; Clark, J. H.; Breeden, S. W. *Catal. Commun.* **2011**, *12*, 993.
13. Verma, S.; Kureshy, R. I.; Roy, T.; Kumar, M.; Das, A.; Khan, N. H.; Abdi, S. H. R.; Bajaj, H. C. *Catal. Commun.* **2015**, *61*, 78.
14. Kim, S.; Sohn, H. J.; Park, S. J. *Curr. Appl. Phys.* **2010**, *10*, 1142.
15. Azar, A. R. J.; Safaei, E.; Mohebbi, S. *Mater. Res. Bull.* **2015**, *70*, 753.
16. Joffres, B.; Lorentz, C.; Vidalie, M.; Laurenti, D.; Quoineaud, A. A.; Charon, N.; Daudin, A.; Quignard, A.; Geantet, C. *Appl. Catal. B Environ.* **2014**, *145*, 167.
17. Kawasaki, T.; Araki, Y.; Hatase, K.; Suzuki, K.; Matsumoto, A.; Yokoi, T.; Kubota, Y.; Tatsumi, T.; Soai, K. *Chem. Commun.* **2015**, *51*, 8742.

18. Zhang, N.; Zhang, Y.; Xu, Y. *J. Nanoscale* **2012**, *4*, 792.
19. Gao, W. *Graphene Oxide: Reduction Recipes, Spectroscopy, and Applications*; Switzerland: Springer International Publishing, **2015**.
20. Liu, Y.; Jin, X. J.; Dionysiou, D. D.; Liu, H.; Huang, Y. M. *J. Power Sources* **2015**, *278*, 773.
21. Su, H.; Wu, S.; Li, Z.; Huo, Q.; Guan, J.; Kan, Q. *Appl. Organomet. Chem.* **2015**, *29*, 462.
22. Li, Z.; Wu, S.; Zheng, D.; Liu, J.; Liu, H.; Lu, H.; Huo, Q.; Guan, J.; Kan, Q. *Appl. Organomet. Chem.* **2014**, *28*, 317.
23. de la Torre, M. J.; Moral, A.; Hernández, M. D.; Cabeza, E.; Tijero, A. *Ind. Crop. Prod.* **2013**, *45*, 58.
24. Nichols, J. M.; Bishop, L. M.; Bergman, R. G.; Ellman, J. A. *J. Am. Chem. Soc.* **2010**, *132*, 12554.
25. Son, S.; Toste, F. D. *Angew. Chem. Int. Ed.* **2010**, *49*, 3791.
26. Sergeev, A. G.; Hartwig, J. F. *Science* **2011**, *332*, 439.
27. Bauer, S.; Sorek, H.; Mitchell, V. D.; Ibáñez, A. B.; Wemmer, D. E. *J. Agric. Food Chem.* **2012**, *06*, 8203.
28. Hummers, W. S Jr.; Offeman, R. E. *J. Am. Chem. Soc.* **1958**, *80*, 1339.
29. Argyropoulos, D. S. *J. Wood Chem. Technol.* **1994**, *14*, 45.
30. Granata, A.; Argyropoulos, D. S. *J. Agric. Food Chem.* **1995**, *43*, 1538.
31. Maurya, M. R.; Titinchi, S. J. J.; Chand, S. *Appl. Catal. A Gen.* **2002**, *228*, 177.
32. Maurya, M. R.; Chandrakar, A. K.; Chand, S. *J. Mol. Catal. A: Chem.* **2007**, *263*, 227.
33. McAllister, M. J.; Li, J. L.; Adamson, D. H.; Schniepp, H. C.; Abdala, A.; Liu, A. J.; Herrera-Alonso, M.; Milius, D. L.; Car, R.; Prud'homme, R. K.; Aksay, I. A. *Chem. Mater.* **2007**, *19*, 4396.
34. Fan, X.; Peng, W.; Li, Y.; Li, X.; Wang, S.; Zhang, G.; Zhang, F. *Adv. Mater.* **2008**, *20*, 4490.
35. Lerf, A.; He, H.; Forster, M.; Klinowski, J. *J. Phys. Chem. B.* **1998**, *102*, 4477.
36. Yuan, B.; Song, L.; Liew, K. M.; Hu, Y. *RSC Adv.* **2015**, *5*, 41307.
37. Ebrahimi, H. P.; Hadi, J. S.; Abdalnabi, Z. A.; Bolandnazar, Z. *Spectrochim. Acta* **2014**, *117*, 485.
38. Boghaei, D. M.; Bezaatpour, A.; Behzad, M. *J. Mol. Catal. A: Chem.* **2006**, *245*, 12.
39. Yamada, S. *Coord. Chem. Rev.* **1999**, *190–192*, 537.
40. Shen, Y.; Xiao, K.; Xi, J.; Qiu, X. *J. Power Sources* **2015**, *278*, 235.
41. Ma, R.; Xu, Y.; Zhang, X. *ChemSusChem* **2015**, *8*, 24.
42. Agarwal, U. P.; Atalla, R. H. In Heitner, C.; Dimmel, D. R.; Schmidt, J. A. Eds. *Lignin and Lignans: Advances in Chemistry*; Taylor and Francis: **2010**, pp 103–136.
43. Lupoi, J. S.; Singh, S.; Parthasarathi, R.; Simmons, B. A.; Henry, R. J. *Renew. Sust. Energy Rev.* **2015**, *49*, 871.